



The Society shall not be responsible for statements or opinions advanced in papers or discussion at meetings of the Society or of its Divisions or Sections, or printed in its publications. Discussion is printed only if the paper is published in an ASME Journal. Authorization to photocopy for internal or personal use is granted to libraries and other users registered with the Copyright Clearance Center (CCC) provided \$3/article or \$4/page is paid to CCC, 222 Rosewood Dr., Danvers, MA 01923. Requests for special permission or bulk reproduction should be addressed to the ASME Technical Publishing Department.

Copyright © 1998 by ASME

All Rights Reserved

Printed in U.S.A.

OPTIMIZATION OF SWIRL BRAKES BY MEANS OF A 3D NAVIER-STOKES SOLVER



K. Krogh Nielsen¹ and
R. A. Van den Braembussche
Turbomachinery Department,
von Karman Institute for Fluid Dynamics,
Rhode-St-Genèse, Belgium

C. M. Myllerup
Machinery Dynamics Group
Ødegaard & Danneskiold-Samsøe A/S
Copenhagen, Denmark

ABSTRACT

This paper deals with the modeling of the flow in the leakage cavity between shroud and stator of a radial pump and the design of optimized swirl brakes at the inlet of the seal. As pressure losses were of no importance in this application, the only criterion for optimization was to minimize the swirl at the seal inlet in order to enhance the rotordynamic stability of it. The design investigation was performed by means of a 3D Navier-Stokes solver. A variety of vane designs were analyzed. It was shown that the three-dimensional vortical structure of the flows plays a dominant role and can be efficiently used to reduce or even invert the swirl at the seal inlet.

INTRODUCTION

The destabilizing effect of swirling flow in narrow internal clearances of radial turbomachinery operating at high pressure is generally acknowledged by turbomachinery designers today (Childs, 1993). An increasing swirl velocity in the direction of rotor rotation creates a circumferential non-uniform pressure field that enhances the whirling motion of the rotor. Deswirl vanes, to reduce the swirl at seal inlet, have a favorable effect on the destabilizing rotordynamic forces. Vanes that facilitate even counter (negative) swirl act stabilizing by counteracting the whirling motion of the rotor (Childs, 1993).

Although deswirl vanes are now widely used, the aerodynamic design of these has not been studied in detail. The results reported in the literature on the swirl brake performance and the flow structures in the vane cavities are very sparse.

The current study intends to provide a better understanding of the flow structures in deswirling vanes and to find out how they should be designed to enhance their stabilizing effect. The numerical method was first validated on test cases by calculating the flow in the vaneless space between rotor and stator. It was followed by a systematic study, in which various designs of deswirl vanes were investigated, to reveal the key parameters and the characteristics of vane design.

NOMENCLATURE

c	=	vane chord
cl	=	vane tip clearance
h	=	vane height
R	=	radial position
s	=	vane pitch
V_{θ}	=	circumferential velocity component
LE	=	leading edge
TE	=	trailing edge

¹ Currently with Ødegaard & Danneskiold-Samsøe A/S, Copenhagen, Denmark

FLOW SOLVER

The simulations performed in this study were done with a modified version of the 3D Navier-Stokes solver TRAF3D. This efficient computer code by Amone (1992) solves the Reynolds averaged Navier-Stokes equations in conservative form on a curvilinear body fitted coordinate system using a cell-centered finite-volume approach.

Local time stepping, residual smoothing and full-approximation-storage multigrid techniques are used to speed up the convergence. The algebraic eddy viscosity model by Baldwin and Lomax (1978) is used for the turbulence closure together with a transition model. This turbulence model is well-proved for boundary layer type flows. For complex applications where the shear layers are not clearly defined the model has some limitations. In recent studies of leakage flows, similar to the present study, the Baldwin and Lomax model was applied successfully (Baskharone and Hensel, 1993 and Baskharone et al., 1994). The modifications of the TRAF3D code relate to the grid generation in complex/narrow geometries between the rotating impeller shroud and the fixed casing wall.

VALIDATION

As it was the first time that the TRAF3D code was used for predicting leakage flows, a validation was initially carried out on relevant geometries for which the results are known.

The first one was a simple smooth straight annular seal for which experimental data were reported by Morrison et al. (1991). The agreement between predictions and measurements was good and improving towards the seal outlet region (Krogh Nielsen, 1997). The small discrepancies in the inlet region could be attributed to admission losses in the test rig that were not modeled in the calculations.

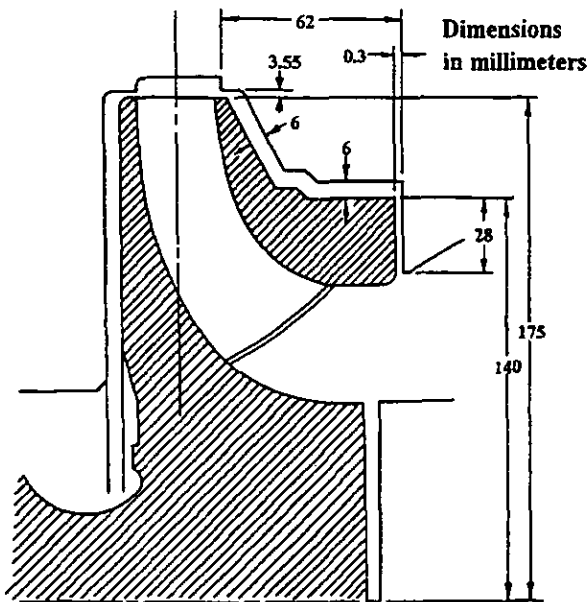


Figure 1. Detailed sketch of impeller and leakage cavity of test case 2.

The second test case was a real pump cavity with large changes in channel orientation and width (Fig. 1). As no detailed flow measurements exist for this geometry, the results were compared with numerical results reported by Baskharone et al. (1994). Very similar flow paths were observed in both predictions with a remarkable agreement between the size and location of the recirculation zones. The last ones result from the large tangential component of the shroud velocity creating strong destabilizing centrifugal forces in the boundary layers. A correct prediction of the recirculation zones was important for the magnitude of the swirl and the flow distribution at the inlet of the seal. The seal inlet swirl profiles were compared and again good agreement was observed. A detailed comparison between the results of both calculations can be found in Krogh Nielsen (1997).

SWIRL BRAKING VANES

A radial seal is rotordynamically stable as a circumferential pressure non-uniformity of the seal pressure field does not create rotordynamic forces. For an axial seal, a non-uniform pressure will lead to rotordynamic forces that may be destabilizing. As the seal inlet swirl is determining the magnitude of the non-uniformity, seal inlet swirl control is vital for axial seal configurations. Therefore, the present study of swirl braking vanes was carried out on a geometry similar to Fig. 1 in which the radial seal was replaced by an axial wear-ring seal. One argument for employing axial seals is that they allow for large axial movements of the rotor.

Figure 2 is an illustration of the cavity geometry considered. The swirl braking vanes were fixed on the outer stator surface with a constant clearance at the inner rotor surface. The long vaneless leakage cavity facilitated realistic flow conditions at the vane inlet.

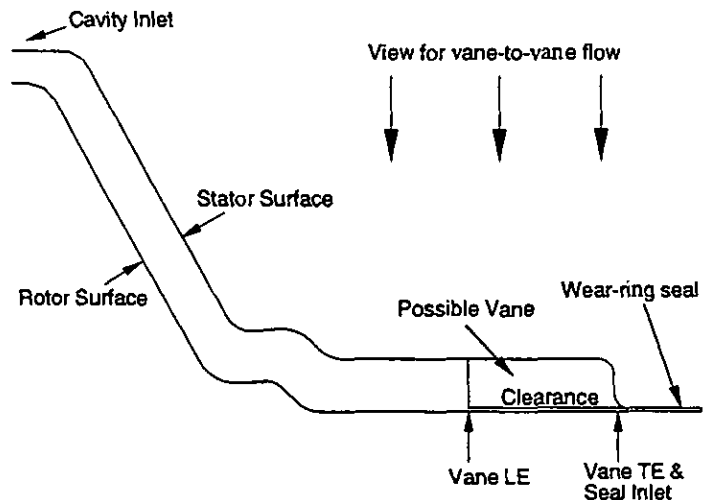


Figure 2. Meridional section of geometry including vanes.

Figure 3 has been included to further clarify the complex geometry and the terminology to be used when discussing the results. The grid lines included do not represent the actual cell number or density.

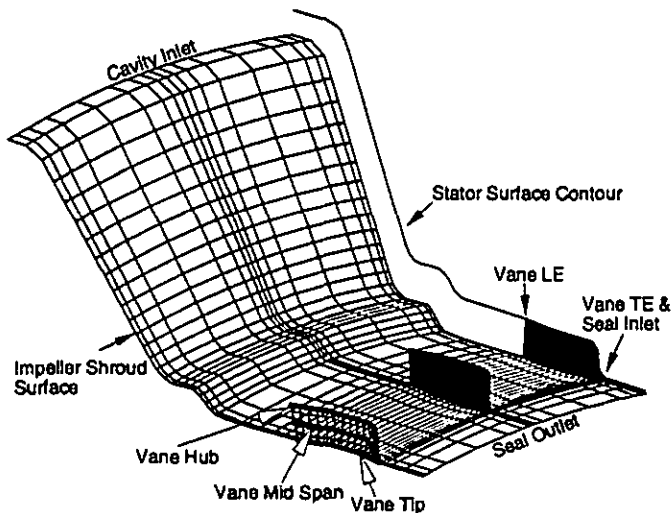


Figure 3. 3D representation of cavity geometry including vanes.

Vane Design Considerations

Swirl braking vanes differ significantly from traditional bladings in several aspects. The meridional flow contraction and deflection effects are very pronounced in cavity flows. The most extreme location is the one where the main cavity flow enters the seal. The flow area contraction in Fig. 2 is 17 to 1. Abrupt meridional flow deflections up to 90° are not uncommon. Viscous effects are very important because of the small tip clearances and flow separation.

Typical non-dimensional profiles of the swirl and meridional velocities just upstream the vane leading edge are given in Fig. 4 to illustrate the vane inlet boundary conditions. The profiles are pitchwise averaged and for both profiles the reference length is the local cavity height and the reference velocity is the local shroud surface velocity.

Seals are designed to control the leakage mass flow. This results in a low meridional velocity in the leakage cavity where the cross section is much larger than in the seal. As a consequence the circumferential flow velocity component in the cavity is normally much larger than the axial one, cf. Fig. 4. In the present cases flow angles, measured against the axial direction, of $80-90^\circ$ were encountered. It is quite obvious that for this highly swirling flow, it is impossible to design vanes that do not cause considerable flow separation without introducing unacceptable high blockage, because of the large number of vanes with finite blade thickness.

Whereas traditional bladings are designed with strong emphasis on low blade losses, a design of deswirling vanes does not have low losses as a main priority. On the contrary, higher losses can even be beneficial in terms of creating an additional pressure drop limiting the overall leakage flow rate.

The vane designs reported in this paper were installed in the axial part of the cavity and were obtained by a systematic variation of what was expected to be relevant parameters. Starting from a baseline design, the design parameters were altered one by one to evaluate their influence on performance.

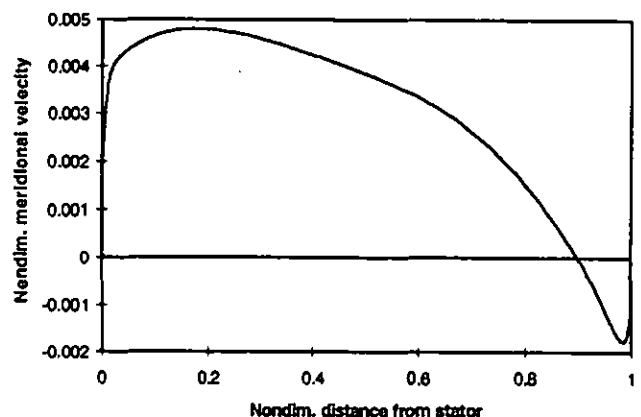
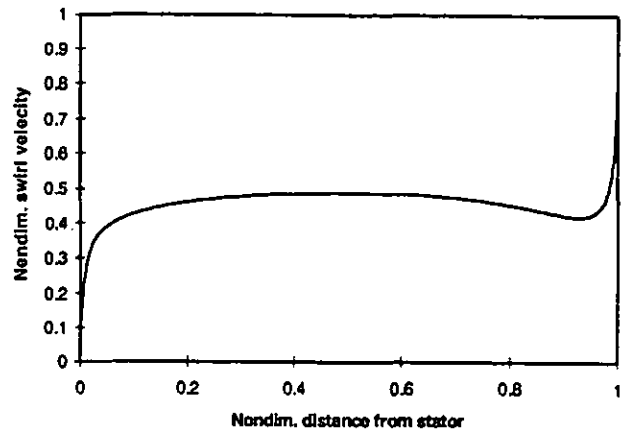


Figure 4. Typical velocity profiles just upstream the vane leading edge.

Assumptions and Boundary Conditions

The inlet boundary conditions for total pressure and flow angles applied to the vane calculations were similar to those applied to the second test case by Baskharone et al. (1994). The conditions used in the present simulations were as reported by Baskharone and Hensel (1993) and Bolleter et al. (1989):

Impeller speed: 2000 rpm
 Impeller tip radius: 0.175 m
 Working medium is water at 30°C
 Leakage mass flow: 3.85 kg/s
 Total impeller head: 68 m
 Tip Reynolds number $8.02 \cdot 10^6$

The outlet static pressure was corrected to obtain the same mass flow for all vane designs.

In all calculations it was assumed that the rotor was located concentric with respect to the stator. The y^+ values of the wall adjacent cells were kept sufficiently small to guarantee a good resolution of the boundary layer. The circumferential extent of the calculation domain was limited to one pitch bay applying periodicity conditions. As the vane designs investigated were sharp nosed, H-grids were applied. Grids with 148, 40, 32 grid points in respectively

the streamwise, radial and vane-to-vane directions were used to discretize the ensemble flow field. As a consequence, the flow field resolution within the seal was very good. Several investigations proved the grid independence of the solutions. The CPU time requirement of a vane design calculation was approximately 5 hours on a DEC 500 5/333 workstation and the convergence stability was good.

Straight Axial Vane Design

The short straight axial vane design, which is presented in Fig. 3, served as a starting geometry for all subsequent modifications. This configuration consists of 40 straight axial vanes that are radial in their spanwise direction resulting in a pitchwise vane spacing of 23 mm at mid-span radius. The vane design investigated extends half of the way from the seal entrance towards the first upstream cavity bend, as shown in Fig. 2.

The clearance between the vane tip and the impeller shroud is 0.72 mm, equivalent to twice the seal clearance. The vane thickness distribution was not given much attention in the current study because the incidence angles are so extreme that flow separation is inevitable. A vane thickness of 2.0 mm was chosen with wedge-shaped leading and trailing edges. To summarize:

- Vane number: 40
- Seal clearance: 0.36 mm
- Pitch to chord ratio (s/c): 1.33
- Aspect ratio (h/c): 0.31
- Clearance ratio (cl/h): 0.11
- Contraction at seal inlet: 17

Figure 5 shows the vane-to-vane flow field at the cavity mid-span upstream of the vanes, inside the vanes and in the seal, seen from the view direction indicated in Fig. 2.

In accordance with the earlier discussions, the inlet flow is close to tangential at the leading edges (LE) of the vanes. This leads to very high incidence angles for the straight axial vanes and massive separation from the suction side is observed. The impinges on the pressure side creating a very large vortex that more or less controls the whole vane-to-vane flow. At the vane suction side the flow moves from the trailing edge (TE) area towards the LE. This recirculation is very beneficial from the point of view of creating counter swirl at the entrance to the seal. Large counter swirl velocities are found at the entrance to the seal, especially in the half part of the vane-to-vane section close to the vane suction side.

At the seal inlet, the flow acceleration is large in the streamwise direction due the narrowness of the seal. In the seal, where no vanes are found, the flow is strongly influenced by the rotation of the impeller shroud surface and therefore experiences a deflection from counter swirling at the inlet to swirling with the rotor at the outlet.

The flow in the vane-to-vane section is highly three-dimensional and varies considerably in the vane spanwise direction. Close to the stator the vane-to-vane vortex is more pronounced as it is less affected by the impeller shroud rotation. Near the vane tip the vortex disappears due to the strong shear stress imposed by the proximity of the rotating shroud.

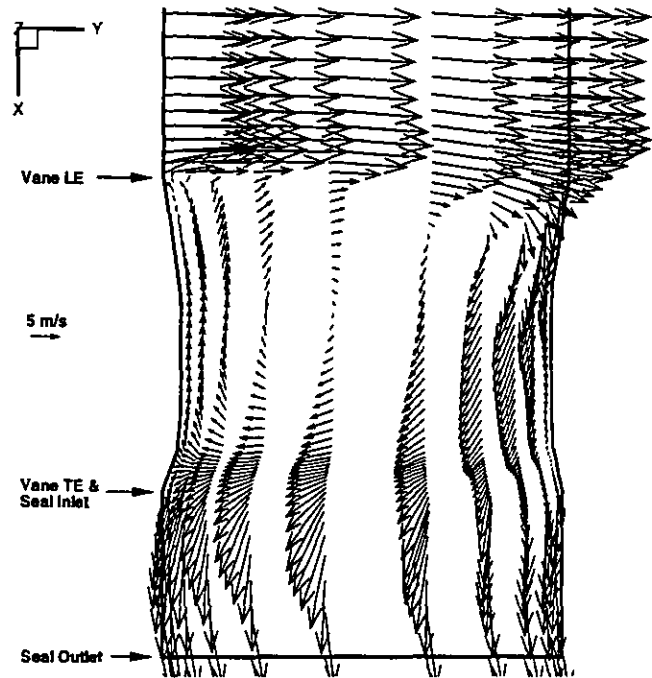


Figure 5. Flow field of baseline design at mid-span.

Figure 6 gives the pitchwise averaged meridional flow field just upstream of and inside the vanes. The figure has been restricted to this important region to facilitate a more detailed investigation of the radial velocities. The contour variable is the swirl velocity that has been non-dimensionalized by the local surface velocity (positive swirl in the direction of the impeller rotation). It should be stressed that the flow field presented is a pitchwise averaged one hiding the large variations in the circumferential direction.

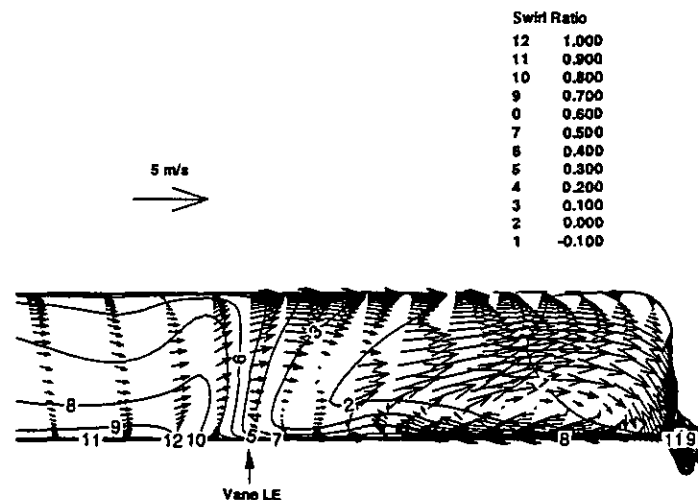


Figure 6. Pitchwise averaged meridional flow field.

Some important flow phenomena are observed. The flow enters the blading mainly in the upper half of the cavity where the swirl velocity is the smallest. The upper flow is deflected downwards along the radial surface and enters the seal. The variation in contour level from the vane leading edge to the trailing edge illustrates the existence of the aforementioned vane-to-vane vortex. The counter

swirling part of the vortex appears in the downstream part of the vane-to-vane flow region.

Adjacent to the rotating shroud surface a vortex is observed just upstream the seal inlet. This pitch averaged seal inlet vortex is very important in terms of reducing the seal inlet swirl as it effectively prevents the highly swirling fluid adjacent to the rotor surface from entering the seal by "pumping" it upstream. Simultaneously, this vortex allows the counter swirling fluid that comes from the upper part of the blading to enter the seal. The upstream moving leg of the vortex is mainly in the clearance whereas the downstream flowing part is within the blading. The contouring shows where the highly swirling fluid lifts off the impeller surface and enters the blading. After moving downstream within the blading the now deswirled fluid impinges on the impeller surface and moves again upstream.

The "swirl ratio" is introduced to quantify the stabilizing effect of the deswirl vanes. It is the mass averaged swirl velocity at the seal inlet, non-dimensionalized by the local peripheral velocity of the rotor surface. In this context, the position of the seal inlet is defined to be the location of the vane trailing edge. The average seal inlet flow of the baseline design is counter swirling, corresponding to a negative swirl ratio of -10%. This should be compared with a positive swirl ratio of 40% in the geometry without deswirl vanes.

Pitch to Chord Ratio

The flow guidance in conventional unseparated cascades is improved by decreasing the pitch to chord ratio. The influence of this ratio on the performance of the swirl braking vanes was investigated in terms of two designs. A decreased ratio was obtained by increasing the vane length at constant vane number. An increased ratio was achieved by reducing the vane number at constant vane chord.

For the low pitch to chord ratio design the vane length was extended to the complete axial part of the cavity. The new pitch to chord and aspect ratios are 0.66 and 0.16, respectively. The mid-span vector field equivalent to Fig. 5 is shown in Fig. 7.

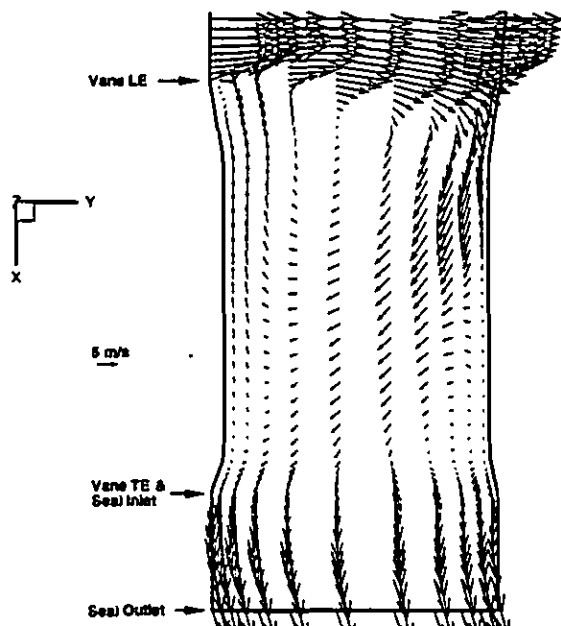


Figure 7. Flow field for low pitch to chord ratio design at mid-span.

The vane-to-vane vortex is seen to be located close to the vane leading edge and the counter swirl part of the vortex does not extend far enough downstream to create a large counter swirl at the seal inlet. The counter swirl at the seal inlet is therefore much weaker than the counter swirl in Fig. 5. The pitch averaged seal inlet vortex is also weaker for this vane design (plot not included), but the change is not as large as could be concluded from the vane-to-vane vortex. Evaluation of the seal inlet swirl ratio gives a positive value of 6% and confirms the unfavorable effect of a decreased pitch to chord ratio.

The influence of an increased pitch to chord ratio was investigated by reducing the vane number to 10, equivalent to a pitch to chord ratio of 5.3. Figure 8 includes a vector plot for the mid-span location, similar to Fig. 5.

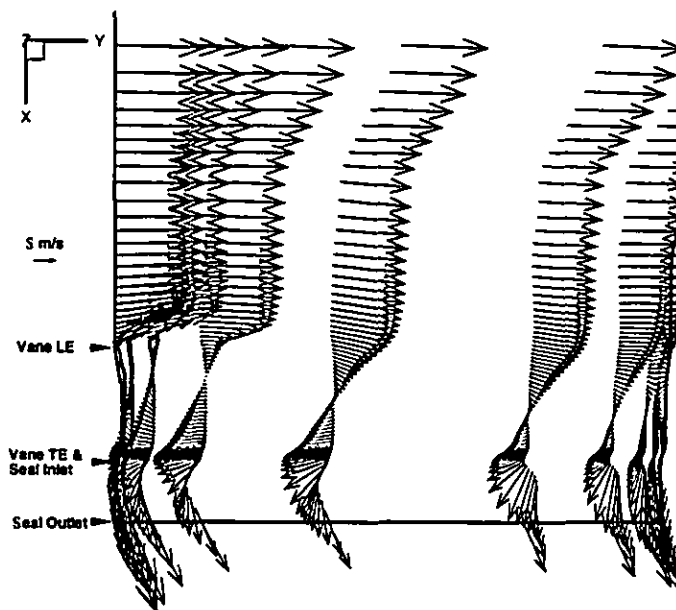


Figure 8. Flow field for high pitch to chord ratio design at mid-span.

Compared with the baseline design, one observes an increased pressure side impingement and a stronger vane-to-vane vortex. Evaluation of the seal inlet swirl ratio gives a value of -15%. This improvement is a direct consequence of the increased vorticity. The increased/decreased flow guidance with decreased/increased pitch to chord ratio is not applicable in the same manner as for attached flows in guide vanes because of strong flow separation.

It can be concluded that the pitch to chord ratio has an important influence on the strength of the vane-to-vane vortex and thereby on the seal inlet counter swirl. In the range of pitch to chord ratios investigated, the vortex strength increases with an increasing pitch to chord ratio.

Clearance

To investigate the influence of the clearance, a vane design, similar to the original one, was analyzed with vanes only extending half of the way from the stator towards the rotor shroud. The corresponding clearance ratio is 1.0. The meridional pitchwise averaged flow field is shown in Fig. 9.

	Swirl Ratio
12	1.000
11	0.900
10	0.800
9	0.700
8	0.600
7	0.500
6	0.400
5	0.300
4	0.200
3	0.100
2	0.000
1	-0.100

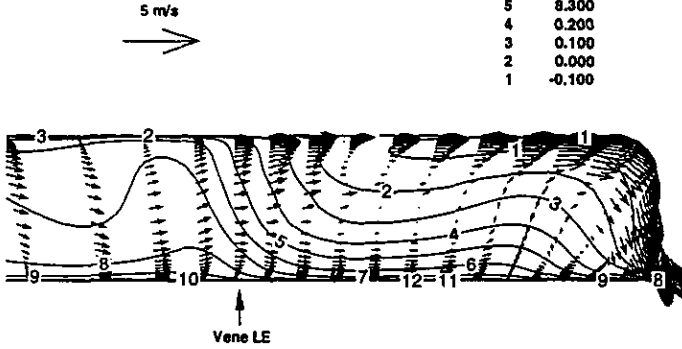


Figure 9. Pitch averaged meridional flow field for large clearance vane design.

For this design the high swirling fluid close to the rotor approaches the seal and increases thereby the swirl level. Fortunately, it is prevented from entering the seal by the seal inlet vortex (Fig. 9). The flow is deflected upwards into the vanes where the vane-to-vane vortex creates a counter swirling velocity component at the seal inlet. A positive seal inlet swirl ratio of 3% is found, illustrating that a large swirl reduction is possible also with a large clearance between the vane tip and the impeller shroud. This finding is very relevant from a manufacturing or rotordynamic point of view.

Streamwise Vane Shape

The purpose of this design is to obtain a larger counter swirl by means of shaped vanes. When bending the vane leading edge in the tangential direction, it is possible to decrease the incidence and improve flow guidance. Introducing a non-zero outlet angle may increase the counter swirl creation at the vane TE. The grid used for these calculations has the inlet and outlet part of the mesh aligned with the vanes.

A design with 45° inlet and -45° outlet angle, measured from the axial direction, was investigated and the mid-span velocity vectors are shown in Fig. 10. Compared with the baseline design, the flow guidance along the vane pressure side has indeed been improved and a positive influence on the strength of the counter swirl at the seal inlet is observed.

A stronger seal inlet vortex is found in the meridional plane (not shown). An evaluation of the swirl ratio gives a value of -14%. One can conclude that a small increase of counter swirl is possible by introducing curved vanes.

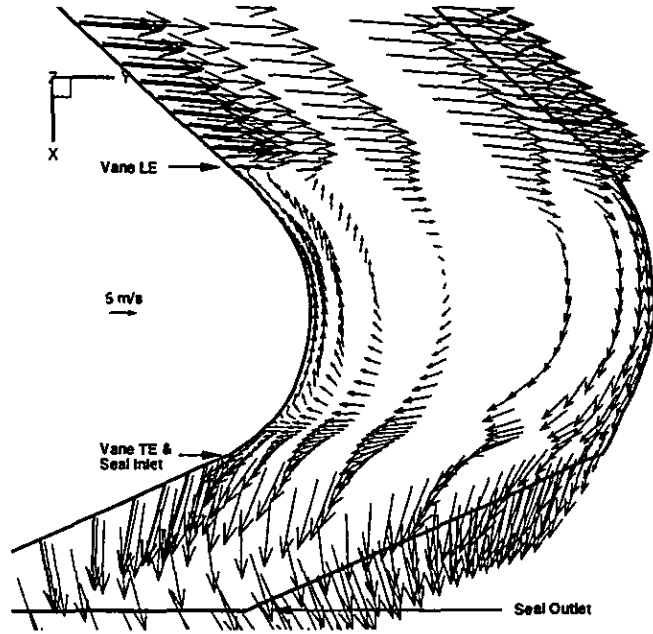


Figure 10. Mid-span flow field for curved vane design.

Vane Lean

The idea of vane lean is to increase the counter swirl of the flow which just upstream of the seal inlet when it moves downwards to enter the seal. Imagine a good guidance of the flow by a large number of radial vanes (0° lean angle). The downward movement will not contribute to the tangential velocity component except for the conservation of tangential momentum ($R \cdot V_\theta = \text{const}$). If on the other hand, the vanes are leaned against the direction of impeller rotation, the downward flow will create a counter swirling velocity component. An interesting flow characteristic is the strong flow acceleration close to the seal inlet which favors attached flow and a good guidance by the leaned vanes. In contrast to the pitch to chord ratio influence described previously, it can be expected that the performance of vane lean will improve with a decreasing pitch to chord ratio.

Figure 11 shows a flow normal plane just upstream of the seal inlet. The view is from the seal in the upstream direction. The vane lean angle is 45°. The flow is seen to be well-guided by the leaned vanes.

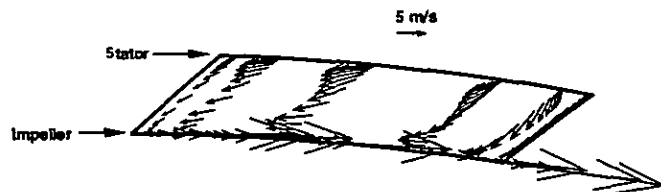


Figure 11. Near-seal flow normal plane.

The average seal inlet swirl ratio for this design is -11%. Compared with the baseline design that showed an average seal inlet ratio of -10%, one can conclude that vane lean seems to be only of secondary importance.

CONCLUSION

The investigations described in this paper clearly show that the flow deflection within swirl braking vanes is governed by vortices and not by conventional flow guidance. This together with the effect of the high losses makes the designs differ from what is normally seen in turbomachinery.

The highly three-dimensional vane flows are characterized by the large vane-to-vane vortex that facilitates the creation of counter swirl at the seal inlet for most of the designs. In the meridional plane the seal inlet vortex is responsible for preventing highly swirling fluid along the impeller shroud from entering the seal. An optimum design is one where the two vortical structures are as large and intense as possible.

Increasing the axial vane length or decreasing the vane number has indicated that there is an optimum value for the pitch to chord ratio. The long axial vane design (small pitch to chord ratio) is too narrow and the vane-to-vane vortex does not extend to the seal inlet. An increasing pitch to chord ratio allows for a larger vane-to-vane vortex to develop and increases the counter swirl.

A large increase in clearance causes the averaged seal inlet swirl ratio to change sign, but the performance degradation is not as severe as could be anticipated.

Curving the vanes, facilitates a larger impingement on the vane pressure side and strengthens the counter swirl.

Vane lean has only a marginal effect on the performance.

Table 1 summarizes the change in swirl ratio with design.

Table 1 Design Results

Vane Design Type	Swirl Ratio Predicted
No Vanes	40%
Baseline Design	-10%
Low Pitch to Chord Ratio	6%
High Pitch to Chord Ratio	-15%
Large Clearance	3%
Streamwise Vane Shape	-14%
Vane Lean	-11%

ACKNOWLEDGMENTS

The support for code modification by Bruno Gouverneur, research engineer at the von Karman Institute, is greatly appreciated.

REFERENCES

Arnone, A., 1992, "Notes on the Use of the TRAF Codes," Technical Report, University of Florence, Italy.

Baldwin, B. S., and Lomax, H., 1978, "Thin-Layer Approximation and Algebraic Model for Separated Turbulent Flows," AIAA paper 78-0257.

Baskharone, E. A., and Hensel, S. J., 1993, "Flow Field in the Secondary, Seal-Containing Passages of Centrifugal Pumps," ASME Journal of Fluids Engineering, Vol. 115, pp. 709.

Baskharone, E. A., Daniel, A. S., and Hensel, S. J., 1994, "Rotordynamic Effects of the Shroud-to-Housing Leakage Flow in Centrifugal Pumps," ASME Journal of Fluids Engineering, Vol. 116, pp. 558-563.

Bolleter, U., Leibundgut, E., and Sturchler, R., 1989, "Hydraulic Interaction and Excitation Forces of High Head Pump Impellers,"

Presented at the Third Joint ASCE/ASME Mechanics Conference, University of California, La Jolla, CA.

Childs, D., 1993, "Turbomachinery Rotordynamics," John Wiley & Sons, Inc., New York.

Krogh Nielsen, K., 1997, "Rotordynamic Impact of Swirl Brakes," Diploma Course Report 1997-28, von Karman Institute for Fluid Dynamics, Rhode-St-Genèse, Belgium.

Morrison, G. L., Johnson, M. C., and Tattersson, G. B., 1991, "Three-Dimensional Laser Anemometer Measurements in an Annular Seal," ASME Journal of Tribology, Vol. 113, pp. 421-427.